Journal of Power Sources 189 (2009) 1147–1153

Contents lists available at ScienceDirect

Journal of Power Sources

journal homepage: www.elsevier.com/locate/jpowsour

# The effect of a Co–Al mixed metal oxide coating on the elevated temperature performance of a $LiMn_2O_4$ cathode material

Zhanxu Yang, Wensheng Yang*, David G. Evans, Yingying Zhao, Xun Wei

*State Key Laboratory of Chemical Resource Engineering, Beijing University of Chemical Technology, 15 Bei San Huan East Road, Beijing 100029, China*

ARTICLE INFO

*Article history:*
Received 15 July 2008
Received in revised form 24 December 2008
Accepted 29 December 2008
Available online 16 January 2009

*Keywords:*
Lithium-ion battery
Cathode material
Spinel
Surface coating
Co–Al mixed metal oxide

ABSTRACT

Co–Al mixed metal oxide (CoAl-MMO) has been used for surface modification of $LiMn_2O_4$ spinel by means of a co-precipitation method in an attempt to improve the electrochemical performance of $LiMn_2O_4$ at elevated temperature. The surface modified materials were characterized by X-ray diffraction (XRD), field emission scanning electron microscopy (FE-SEM), energy dispersive X-ray spectrometry (EDS), Auger electron spectroscopy (AES) and galvanostatic charge–discharge cycling. After heat-treatment at 400 °C, the CoAl-MMO coated $LiMn_2O_4$ shows better capacity retention at both 25 °C and 55 °C than the pristine $LiMn_2O_4$. The enhancement in electrochemical performance is mainly attributed to the CoAl-MMO coating layer which has the synergistic effect of cobalt and aluminum oxide species and could block the direct contact between the spinel cathode material and electrolyte resulting in Mn dissolution decrease.



## 1. Introduction

$LiMn_2O_4$ has been considered as a potential alternative to $LiCoO_2$ for use as the positive electrode in rechargeable Li-ion battery because of its low cost, low toxicity and high safety [1–3]. However, $LiMn_2O_4$ shows poor cycling performance at elevated temperatures [4,5]. Although the reason for the poor cycling performance is not fully understood, several possible mechanisms have been suggested including Mn dissolution, Jahn–Teller distortion, and changes in crystallinity [2–8].

To overcome the shortcomings of $LiMn_2O_4$, several approaches such as ion (cation or anion) substitution and surface treatment have been carried out. Although ion substitution can improve the stability of the spinel structure, and suppress the Jahn–Teller distortion, studies indicate the dissolution of Mn occurs mainly at the interface between spinel $LiMn_2O_4$ and electrolyte [9–11]. Therefore, surface modification with various metal oxides [12–15], such as $Al_2O_3$, $Co_3O_4$, or ZnO, is considered as one effective method to solve the problem, because these oxides can suppress Mn dissolution by scavenging HF from the electrolyte. However, to the best of our knowledge, there are no reports on the use of a mixed metal oxide (MMO) as a coating material. It is expected that mixed metal oxides will have the combined advantages of their individual metal oxide components and synergistic interactions which may afford enhancement of the electrochemical performance of coated cathode materials.

In this paper, we report for the first time the enhancement in electrochemical performance of $LiMn_2O_4$ by coating with a Co–Al mixed metal oxide (CoAl-MMO). The mixed metal oxide was prepared from a Co–Al layered double hydroxide (CoAl-LDH) precursor; this has a uniform distribution of metal cations on the atomic level, which affords a mixed metal oxide with a more uniform distribution of cobalt and aluminum than can be obtained by conventional methods [16]. Here we study the effects of different calcination temperatures and amounts of coatings on the structure, morphology and electrochemical cycling performance of CoAl-MMO coated $LiMn_2O_4$ at 25 °C and 55 °C.

## 2. Experimental

### 2.1. Synthesis of materials

Pristine $LiMn_2O_4$ powder with an initial discharge specific capacity of about 100 mAh $g^{-1}$ was provided by Shijiazhuang Best Battery Material Co., Ltd. (China). The required amount of $LiMn_2O_4$ was first suspended in distilled water with vigorous agitation. A solution containing $Co(NO_3)_2{\cdot}6H_2O$ and $Al(NO_3)_3{\cdot}9H_2O$ was then slowly added drop-wise to the $LiMn_2O_4$ suspension. At the same time, a solution containing $LiOH{\cdot}H_2O$ was added drop-wise in order to maintain the mixture at pH 10.5. The suspension was subsequently aged at room temperature with vigorous agitation for 3 h. The final powder was filtered and dried at 120 °C for 12 h, and

* Corresponding author. Tel.: +86 10 6443 5271; fax: +86 10 6442 5385.
*E-mail address:* yangws@mail.buct.edu.cn (W. Yang).

0378-7753/$ – see front matter © 2009 Elsevier B.V. All rights reserved.
doi:10.1016/j.jpowsour.2008.12.152

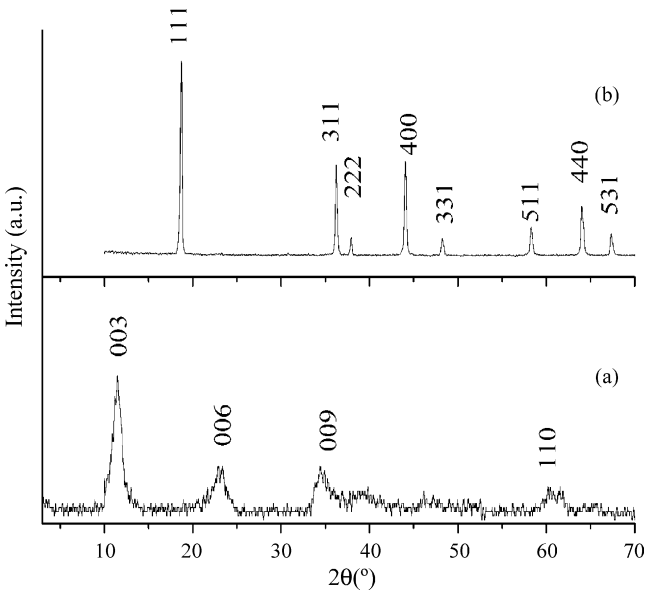


**Fig. 1.** XRD patterns of (a) the CoAl-LDH precursor and (b) CoAl-LDH coated $LiMn_2O_4$.

subsequently heat-treated in a furnace at different temperatures for 5 h in air. Pure LDH ($[M^{II}_{1-x}M^{III}_x(OH)_2]^{x+}[A^{n-}]_{x/n}\cdot yH_2O$) phases can only be formed for stoichiometries in the range $0.20 < x < 0.33$, i.e. $M^{II}/M^{III}$ ratios in the range 2–4 [17]. Therefore, the amount of Co in the coating solution was varied from 2 wt.% to 4 wt.% (based on $LiMn_2O_4$), while the amount of Al in the coating solution was fixed at 0.5 wt.% (based on $LiMn_2O_4$). To compare with the CoAl-MMO coating material, the $Co_3O_4$ coated $LiMn_2O_4$ was prepared by the above method, and the amount of Co in the coating solution was fixed at 3 wt.% (based on $LiMn_2O_4$).

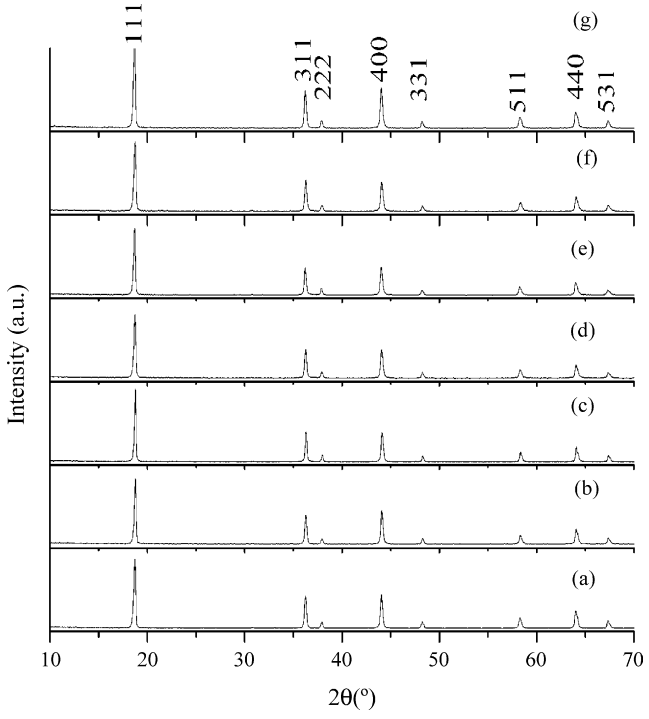


**Fig. 2.** XRD patterns of (a) the pristine $LiMn_2O_4$ and CoAl-MMO (3 wt.% Co and 0.5 wt.% Al based on $LiMn_2O_4$) coated $LiMn_2O_4$ calcined at (b) 300 °C, (c) 400 °C, (d) 500 °C, (e) 600 °C, (f) 700 °C and (g) 800 °C for 5 h.

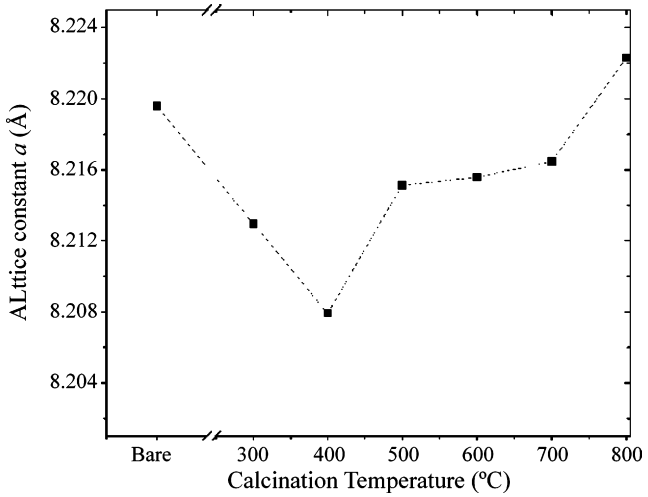


**Fig. 3.** Values of the unit cell parameter $a$ of the pristine $LiMn_2O_4$ and CoAl-MMO (3 wt.% Co and 0.5 wt.% Al based on $LiMn_2O_4$) coated $LiMn_2O_4$ calcined at different temperatures for 5 h in air.

### 2.2. Characterization of materials

The structures of the products were analyzed by powder X-ray diffraction (XRD), using a Shimadzu XRD-6000 diffractometer operated at 40 kV and 30 mA from 10° to 70° at the wavelength of Cu Kα radiation (λ = 0.15406 nm). The particle morphologies of the products were observed using a field emission scanning electron microscope (FE-SEM) (Hitachi S4700). The chemical composition on the surface of the cathode materials was examined by energy dispersive X-ray spectrometry analysis (EDS) (EDAX GENESIS 60). Auger electron spectroscopy (AES) (ULVAC-PHI, AES-PHI 700) was used to examine the spatial distribution of constituent ions in the coated particles. Mn dissolution content of the sample after storage in electrolyte for 24 h at 55 °C was examined by inductively coupled plasma-atomic emission spectroscopy (ICP-AES) (Shimadzu ICPS-7500).

Electrochemical behaviors during charge/discharge cycles were examined using a two-electrode test cell with lithium foil as the negative electrode. A positive electrode was made by coating a paste of active material, acetylene black and polyvinylidene fluoride (PVDF) binder (90:5:5, wt.%) on an aluminum-foil collector. The positive film was subjected to roll press and electrodes of 10 mm diameter were punched out. The positive electrodes were dried at 110 °C for 12 h in a vacuum oven. Coin-type cells (CR 2032) were assembled in an argon filled glove box with an electrolyte of 1 mol $L^{-1}$ $LiPF_6$ in EC–EMC–DMC (1:1:1, volume ratio) solution and a separator of Celgard 2400. The electrochemical data were collected using LAND CT2001A test system within the potential range of 3.0–4.35 V (vs. $Li^+/Li$) at a constant current density of 0.2 mA $cm^{-2}$.

## 3. Results and discussion

After precipitation of a solution containing $Co(NO_3)_2\cdot 6H_2O$ and $Al(NO_3)_3\cdot 9H_2O$ and a solution of $LiOH\cdot H_2O$, the precipitate was dried at 120 °C. The XRD pattern of the product exhibits the characteristic diffraction peaks of a well-crystallized hydrotalcite-like LDH material as shown in Fig. 1a. The CoAl-LDH coated $LiMn_2O_4$ was prepared by the same process to synthesize the LDH material. The XRD pattern of the CoAl-LDH coated $LiMn_2O_4$ material does not show any additional peaks other than those of $LiMn_2O_4$ (Fig. 1b). This is presumably because the content of CoAl-LDH is low and CoAl-LDH forms only a thin film on the surface of $LiMn_2O_4$.

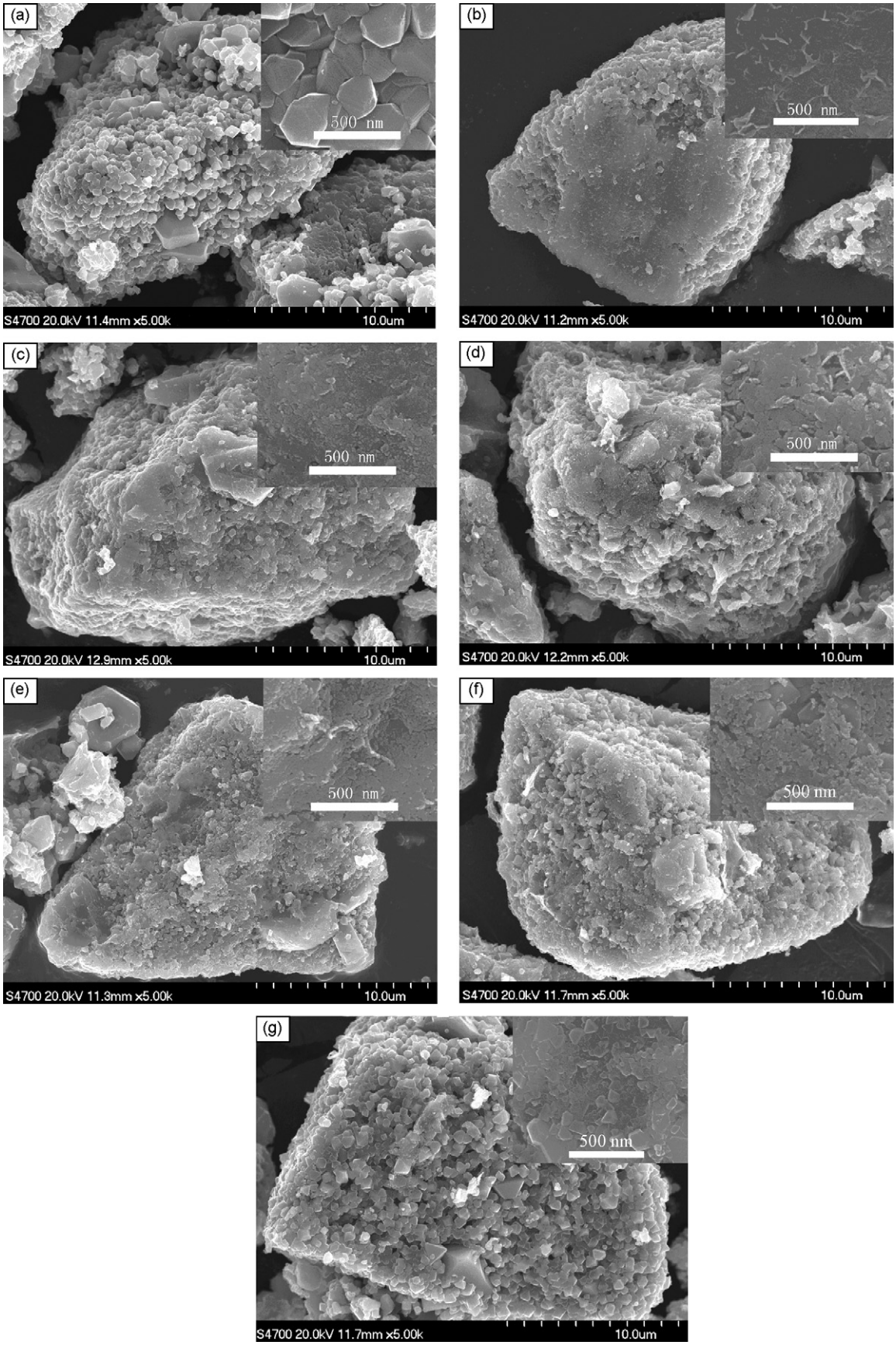


**Fig. 4.** FE-SEM micrographs of (a) the pristine $LiMn_2O_4$ and CoAl-MMO (3 wt.% Co and 0.5 wt.% Al based on $LiMn_2O_4$) coated $LiMn_2O_4$ calcined at (b) 300 °C, (c) 400 °C, (d) 500 °C, (e) 600 °C, (f) 700 °C and (g) 800 °C for 5 h. The inset is the corresponding FE-SEM image of the cathode surface at high magnification.

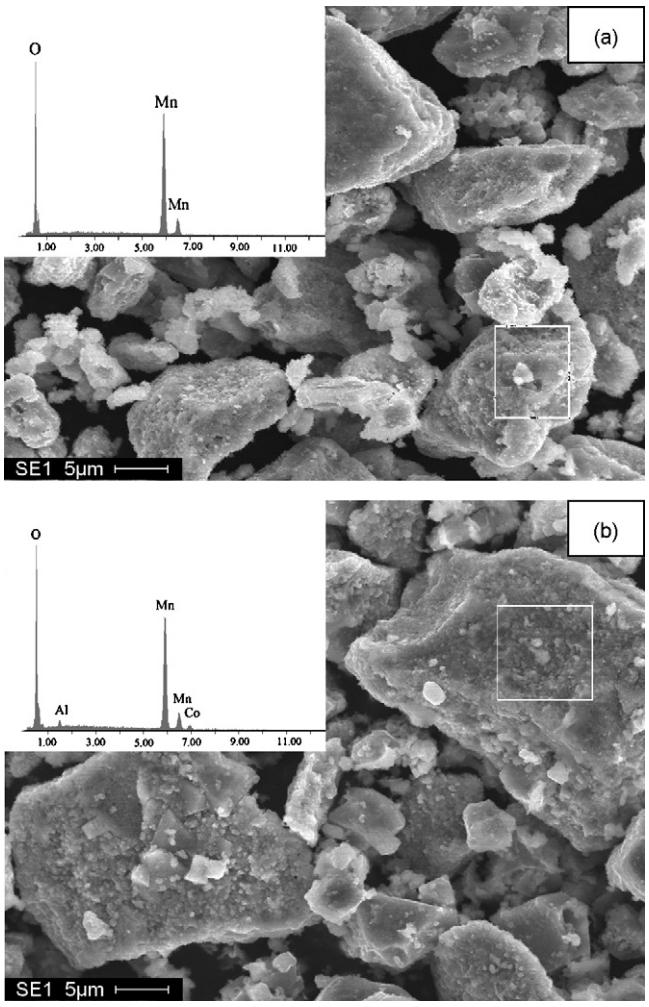


**Fig. 5.** FE-SEM images of (a) the pristine $LiMn_2O_4$ and (b) CoAl-MMO (3 wt.% Co and 0.5 wt.% Al based on $LiMn_2O_4$) coated $LiMn_2O_4$ calcined at 400 °C for 5 h. The inset is the corresponding EDS analyses in the selected region.

The CoAl-MMO coated $LiMn_2O_4$ was prepared by calcining the CoAl-LDH coated $LiMn_2O_4$ material. The XRD patterns of the pristine $LiMn_2O_4$ (Fig. 2a) and CoAl-MMO (3.0 wt.% Co and 0.5 wt.% Al based on $LiMn_2O_4$) coated $LiMn_2O_4$ powders calcined at different temperatures (Fig. 2b–g) can all be indexed to a cubic spinel structure with the space group *Fd3m*. The XRD patterns of the CoAl-MMO coated $LiMn_2O_4$ samples do not show any additional peaks other than those of $LiMn_2O_4$. The lattice parameter *a* of the CoAl-MMO coated $LiMn_2O_4$ materials is calculated and is plotted as a function of calcination temperature in Fig. 3. The lattice parameter *a* of the material calcined at 300 °C is significantly smaller than that of pristine $LiMn_2O_4$. This can be attributed to Co and Al diffusing into the $LiMn_2O_4$ lattice; because the ionic radii of cobalt ($Co^{3+}$, 0.545 Å) and aluminum ions ($Al^{3+}$, 0.535 Å) are smaller than that of manganese ($Mn^{3+}$, 0.645 Å), a decrease in unit cell parameter is therefore expected. In addition, the Co–O and Al–O bond energies are larger than that of Mn–O, which results in a stabilization of the spinel structure [18–21]. Increasing the calcination temperature to 400 °C leads to a further decrease in lattice parameter, consistent with increased incorporation of Co and Al. So Co and Al ions near the bulk $LiMn_2O_4$ would diffuse into the $LiMn_2O_4$ lattice to form a solid-solution $LiMn_{2-x-y}Co_xAl_yO_4$ phase during the calcination process. However, when the calcination temperature is increased to 500 °C or above, the lattice parameter *a* increases. This can be attributed to oxygen loss from the spinel structure which becomes more significant with increasing heating temperature [22,23]. Such loss of oxygen would affect the composition and structure of the spinel compound. In order to maintain the charge balance in $LiMn_2O_4$, oxygen loss causes reduction of $Mn^{4+}$ to $Mn^{3+}$. This results in a decrease in the attractive force between the Mn and O ions and, therefore, an expansion in unit cell volume.

Fig. 4 presents the FE-SEM images of the pristine $LiMn_2O_4$ and CoAl-MMO (3.0 wt.% Co and 0.5 wt.% Al based on $LiMn_2O_4$) coated $LiMn_2O_4$ materials calcined at different temperatures. The surface morphologies of the CoAl-MMO coated $LiMn_2O_4$ after heat-treatment below 800 °C are different from those of the pristine one at low magnification. When the heat-treatment is increased to 800 °C, the particle morphology of the coated cathode material is similar to that of the pristine one at low magnification. This above change process is mainly due to the process of CoAl-LDH decomposition at different temperatures. When the CoAl-LDH is calcined below 200 °C, it would release the interlayer water and the partial dehydroxylation of the metal hydroxide layers. A further increase in calcination temperature, the interlayer anion would be released and the layered structure of the metal hydroxide layer would collapse to form poorly crystalline mixed metal oxide [16,24]. Moreover, the surface morphology of the coated cathode material after heat-treatment changes obviously at high magnification. Comparison of the images for the pristine $LiMn_2O_4$ and coated $LiMn_2O_4$ implies that there is a coating layer on the surface of the $LiMn_2O_4$. In order to confirm this, EDS analyses in the selected region were performed as shown in Fig. 5. Cobalt and aluminum can be clearly observed on the surface of modified $LiMn_2O_4$ while the pristine sample does not exhibit any cobalt and aluminum.

The changes in lattice parameter *a* and morphology described above suggest that increasing heat-treatment temperature results in diffusion of Co and Al ions to an increasing depth. Since the

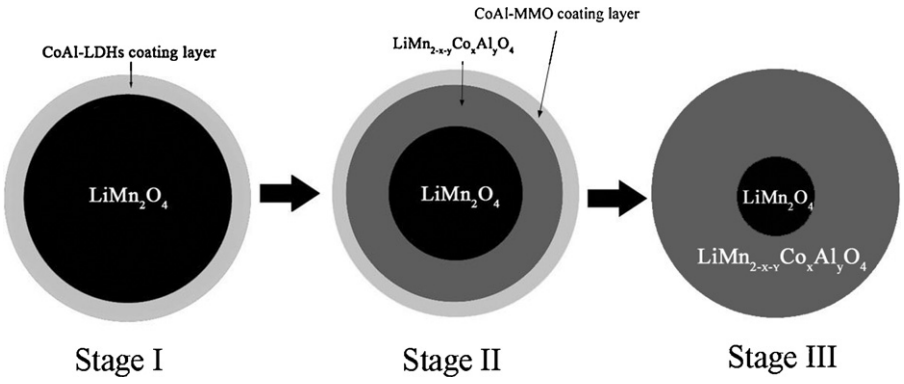


**Fig. 6.** Schematic illustration for the structure of coated $LiMn_2O_4$ particle prior to calcination (left) and after calcination at different temperatures. The heat-treatment temperature range of stages II and III at low calcination temperature and at high calcination temperature, respectively.

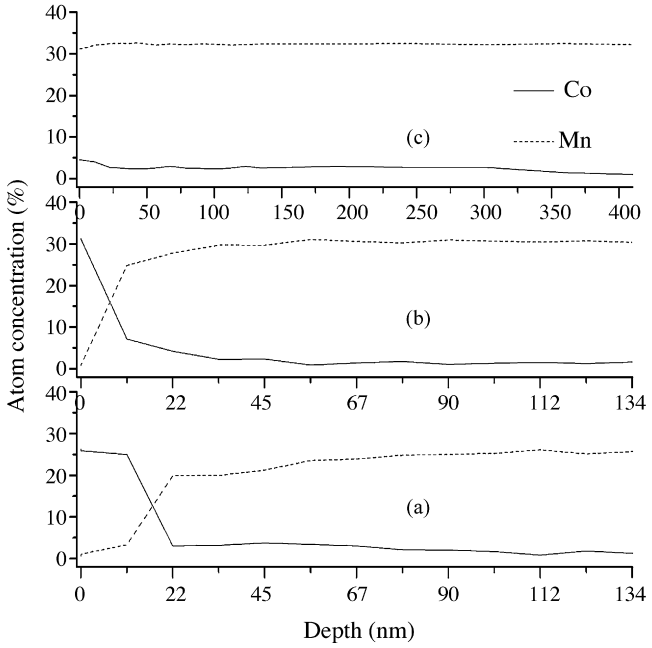


**Fig. 7.** Depth profiles of coated $LiMn_2O_4$ particle (a) before calcination, (b) calcination at low temperature (400 °C) and (c) calcination at high temperature (800 °C) determined by AES.

total Co and Al content in all the modified materials is constant, an increased diffusion depth of Co and Al implies that the proportion of $LiMn_{2-x-y}Co_xAl_yO_4$ near the surface formed by inter-diffusion between the bulk $LiMn_2O_4$ and CoAl-MMO becomes higher and the amount of CoAl-MMO on the surface of $LiMn_2O_4$ decreases. On the basis of the above discussion, the proposed structures of coated $LiMn_2O_4$ particles before calcination and after calcination at different temperatures are illustrated schematically in Fig. 6. The heat-treatment temperature range of stages II and III is at low calcination temperature (about 400 °C) and at high calcination temperature (about 800 °C), respectively. In order to prove the above analysis, AES was carried out to examine the spatial distribution of Co atoms near the surface of the coated particles, and the results are shown in Fig. 7. It can be clearly seen (Fig. 7a) that Mn is hardly detected on the top surface of the coated $LiMn_2O_4$ particles before calcination, which means that $LiMn_2O_4$ particles are completely encapsulated. The Co concentration is high and almost unchanged above a depth of about 11 nm and then decreases sharply below a depth of about 22 nm, whilst the Mn concentration shows the opposite trend, as shown in Fig. 7a. Therefore, the maximum thickness of the coated $LiMn_2O_4$ particles before calcination is about 22 nm, and the coating elements hardly diffuse into the bulk $LiMn_2O_4$ because the drying temperature is only 120 °C. During the low temperature (400 °C) calcination process, the Co concentration on the top surface of the coated $LiMn_2O_4$ particles is initially very high, decreases sharply before a depth of about 11 nm, and then decreases slowly and levels off at a depth of about 56 nm, as shown in Fig. 7b. However, Mn is hardly detected on the top surface of the coated $LiMn_2O_4$ particles during the low temperature calcination process and the Mn concentration shows the opposite trend to the Co concentration, as shown in Fig. 7b. Therefore, the maximum thickness of CoAl-MMO coating layer is about 11 nm and the coating elements diffuse into the bulk $LiMn_2O_4$ during the low temperature calcination process to form an $LiMn_{2-x-y}Co_xAl_yO_4$ phase with a thickness of about 45 nm. Fig. 7c shows that on the top surface of the coated $LiMn_2O_4$ after high temperature (800 °C) calcination, the surface of the sample contains Mn. The Mn content gradually increases with depth, whilst the Co content gradually decreases with depth

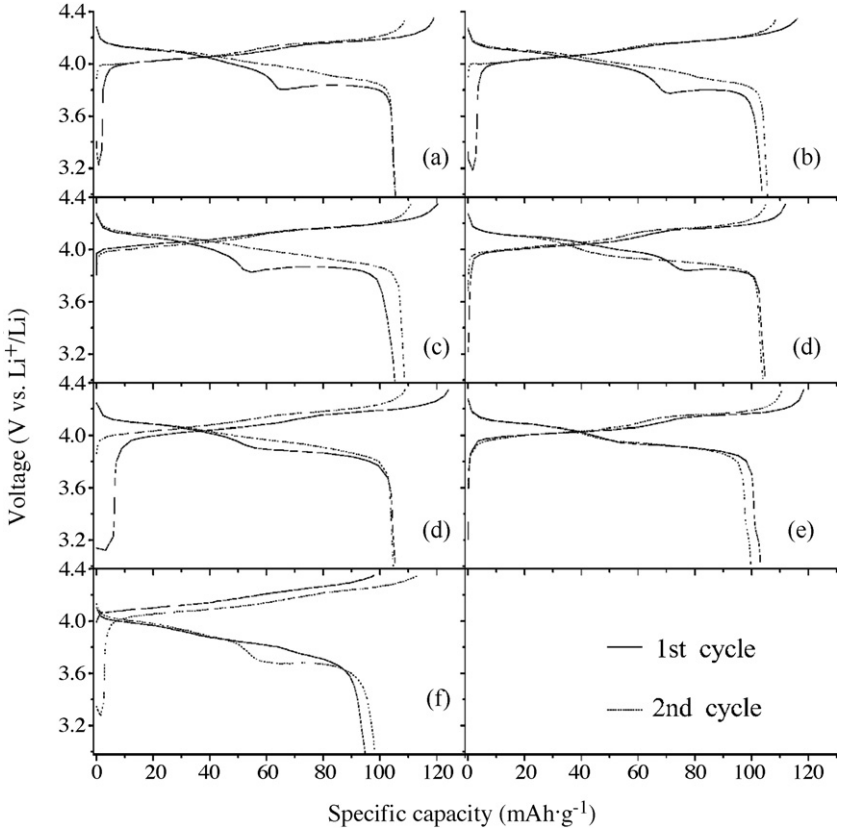


**Fig. 8.** The charge/discharge curves at 25 °C for the first and second cycles of (a) the pristine $LiMn_2O_4$ and CoAl-MMO coated $LiMn_2O_4$ calcined at (b) 300 °C, (c) 400 °C, (d) 500 °C, (e) 600 °C, (f) 700 °C and (g) 800 °C for 5 h.

**Table 1**
Mn dissolution amounts of the pristne $LiMn_2O_4$ and CoAl-MMO coated $LiMn_2O_4$ (3.0 wt.% Co and 0.5 wt.% Al based on $LiMn_2O_4$) which have been immersed in electrolyte of 1 mol $L^{-1}$ $LiPF_6$ in EC–EMC–DMC (1:1:1, volume ratio) solution for 24 h at 55 °C.

| Sample | $LiMn_2O_4$ | CoAl-MMO coated $LiMn_2O_4$ |
|---|---|---|
| The amount of Mn dissolution in electrolyte (mg) | 0.204 | 0.058 |

and is below the detection limit at 350 nm. This implies that an $LiMn_{2-x-y}Co_xAl_yO_4$ solid solution is formed on the surface of the cathode material with a thickness of about 350 nm.

Many studies showed that the capacity loss of the spinel were associated with Mn dissolution [4,20,21,25]. To analyze the Mn dissolution behavior in the product, the spinel $LiMn_2O_4$ (0.30 g) and CoAl-MMO coated $LiMn_2O_4$ (0.30 g) (3.0 wt.% Co and 0.5 wt.% Al based on $LiMn_2O_4$) were immersed in 30 mL electrolyte solution (1 mol $L^{-1}$ $LiPF_6$ in EC–EMC–DMC (1:1:1, volume ratio)) for 24 h at 55 °C, and the Mn content was determined by ICP-AES. The ICP analysis results for the pristine and CoAl-MMO coated $LiMn_2O_4$ dissolution into electrolyte are given in Table 1. As shown in this table, the dissolved Mn content of coated sample is much lower than that of the pristine spinel. The result illustrates that CoAl-MMO coated $LiMn_2O_4$ can effectively reduce the dissolution of spinel into the electrolyte.

The cycling stability of the pristine $LiMn_2O_4$ and CoAl-MMO (3.0 wt.% Co and 0.5 wt.% Al based on $LiMn_2O_4$) coated $LiMn_2O_4$ calcined at different temperatures was examined in the potential range 3.0–4.35 V (vs. $Li^+/Li$) at a constant current density of 0.2 mA $cm^{-2}$. The charge/discharge curves at 25 °C for the first and second cycles of the pristine $LiMn_2O_4$ and CoAl-MMO coated $LiMn_2O_4$ calcined at different temperatures are shown in Fig. 8, and the cycling curves at 25 °C and 55 °C are shown in Fig. 9. The pristine $LiMn_2O_4$ delivers an initial discharge specific capacity of 105.6 mAh $g^{-1}$ which decays to 97.4 mAh $g^{-1}$ after 50 cycles at 25 °C. The initial discharge specific capacities of the CoAl-MMO coated $LiMn_2O_4$ materials calcined below 600 °C are all about 105 mAh $g^{-1}$, similar to that of the pristine $LiMn_2O_4$. However, the electrochemical cycling stabilities at 25 °C of the CoAl-MMO coated $LiMn_2O_4$ calcined below 600 °C are slightly enhanced, with the values remaining above 100 mAh $g^{-1}$ after 50 cycles. However, for higher calcination temperature the cycling behavior of modified $LiMn_2O_4$ gradually deteriorates and when the calcination temperature was increased to 800 °C, a drastic capacity fading was observed over 50 cycles. The main reason for this drastic capacity fading is that the destruction of the material structure due to the oxygen losses is severe at high calcination temperature, which can be proved by the extra discharge plateau about 3.2 V in the discharge curves, as shown in Fig. 8e. Deng et al. and Xia et al. have also reported that the oxygen stoichiometry can also be identified by the extra discharge plateau about 3.2 V appearing in the discharge curve for $LiMn_2O_4$ [26–28]. Another possibility is that the surface of the modified sample formed $LiMn_{2-x-y}Co_xAl_yO_4$ solid solution at high calcination temperature which could not block the direct contact between cathode material and electrolyte. Capacity fading is accelerated at 55 °C, as is typical for this family of materials, with the pristine spinel losing about 31% of its initial capacity after 50 cycles. The electrochemical cycling stabilities at 55 °C of the CoAl-MMO coated $LiMn_2O_4$ show a similar variation with calcination temperature to the stabilities at 25 °C. The CoAl-MMO coated $LiMn_2O_4$ calcined at 400 °C has the best cycling stability after 50 cycles at 55 °C, retaining a discharge specific capacity of 92.2 mAh $g^{-1}$ (89.3% retention); this is much higher than that of the pristine $LiMn_2O_4$ (73.7 mAh $g^{-1}$). On the basis of the above results, we suggest that the capacity of the electrode is stabilized because the presence of CoAl-MMO on the surface of the $LiMn_2O_4$ leads to Mn dissolution decrease because of blocking the direct contact between cathode material and electrolyte, which is regarded as one of the most important causes of the capacity loss of $LiMn_2O_4$ at higher temperature [11–14].

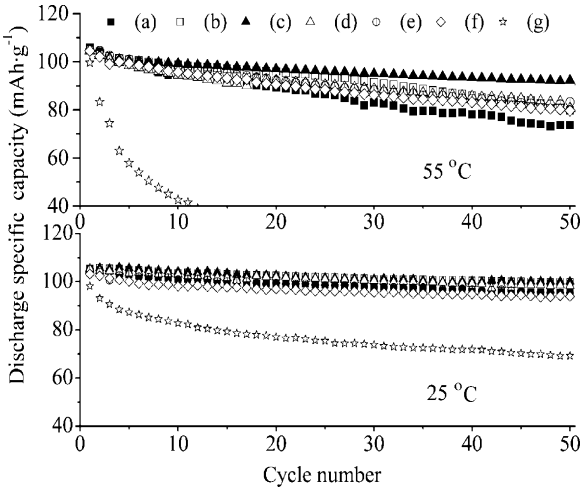


**Fig. 9.** Cycling performances at 25 °C and 55 °C of (a) the pristine $LiMn_2O_4$ and CoAl-MMO (3 wt.% Co and 0.5 wt.% Al based on $LiMn_2O_4$) coated $LiMn_2O_4$ calcined at (b) 300 °C, (c) 400 °C, (d) 500 °C, (e) 600 °C, (f) 700 °C and (g) 800 °C for 5 h.

The heat-treatment temperature of CoAl-MMO coated $LiMn_2O_4$ is a key factor in maximizing the improvement in capacity retention because the electrochemical performance is strongly related to the surface composition and crystal structure. Low temperature heat-treatment is insufficient to significantly improve the cycling stability because the forces between the coating layer and the bulk $LiMn_2O_4$ are weak. With increasing heat-treatment temperature, the coating layer becomes denser and the forces become stronger. However, if the heat-treatment temperature is too high, the surface of the cathode material would form solid solution $LiMn_{2-x-y}Co_xAl_yO_4$ phase which could not block the direct contact between cathode material and electrolyte. Moreover, high calcination temperature leads to oxygen loss that gradually destroys the spinel structure. Therefore, there is an optimal intermediate heat-treatment temperature to form the coating film, which should not only block the direct contact between cathode material and electrolyte but also avoid the destruction of the material structure. In this work, the optimal calcination temperature was found to be 400 °C for CoAl-MMO coated $LiMn_2O_4$. So the heat-treatment temperature was fixed at 400 °C for subsequent studies of the effect of varying the amount of the CoAl-MMO coating on $LiMn_2O_4$.

Fig. 10 shows the XRD patterns of the pristine $LiMn_2O_4$ and $LiMn_2O_4$ coated with CoAl-MMO containing different loadings of cobalt after calcination at 400 °C for 5 h. All the powders were found to consist of a well-defined spinel phase without any other crystalline phase.

The cycling behaviors of the cathode materials were studied as a function of the loading of the CoAl-MMO coating. Fig. 11 shows the cycling performance in the potential range 3.0–4.35 V (vs. $Li^+/Li$) at a constant current density of 0.2 mA $cm^{-2}$ at 25 °C and 55 °C of the pristine $LiMn_2O_4$, CoAl-MMO coated $LiMn_2O_4$ with different CoAl-MMO loadings and $Co_3O_4$ coated $LiMn_2O_4$ with cobalt loading of 3% calcined at 400 °C for 5 h, respectively. The capacity retention of the CoAl-MMO coated $LiMn_2O_4$ after 50 cycles at 25 °C or 55 °C varies with cobalt loading as follows: 3 wt.% > 4 wt.% > 2 wt.%. Although an increase in cobalt loading from 2 wt.% to 3 wt.% is beneficial, larger amounts do not produce any further enhancement and can actually lower the discharge specific capacity because the amount of the electrochemical inactive material increases and the coating layer becomes thicker that it would obstruct the transportation of lithium ion resulting in poor cycling performance. Moreover, the

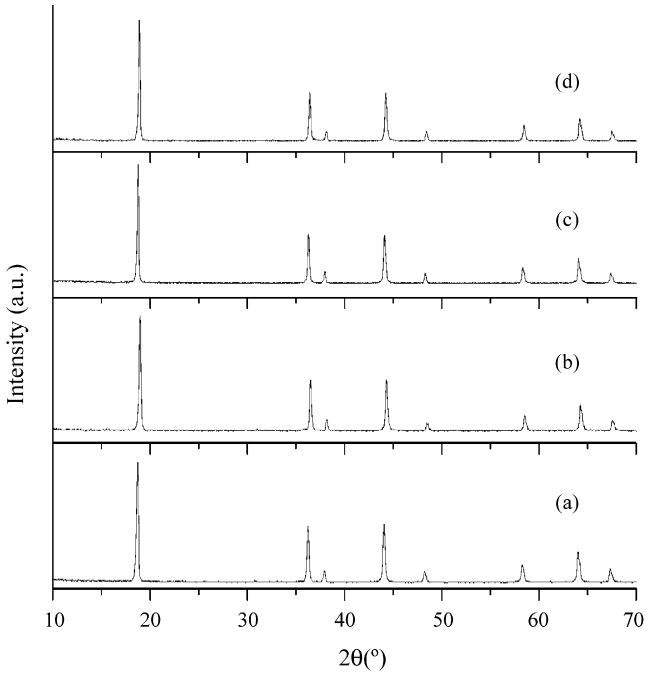


**Fig. 10.** XRD patterns of (a) the pristine $LiMn_2O_4$ and CoAl-MMO coated $LiMn_2O_4$ with cobalt loadings of (b) 2 wt.%, (c) 3 wt.% and (d) 4 wt.% calcined at 400 °C for 5 h.

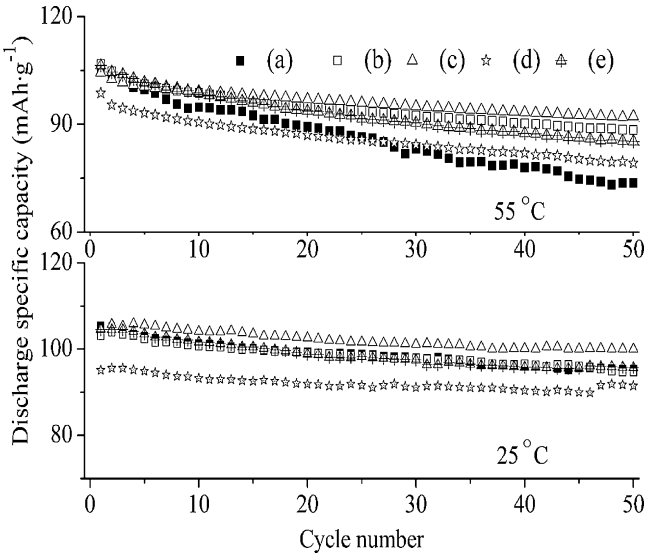


**Fig. 11.** Cycling performances at 25 °C and 55 °C of (a) the pristine $LiMn_2O_4$, CoAl-MMO coated $LiMn_2O_4$ with cobalt loadings of (b) 2 wt.%, (c) 3 wt.% and (d) 4 wt.%, and (e) $Co_3O_4$ coated $LiMn_2O_4$ with cobalt loading of 3% calcined at 400 °C for 5 h, respectively.

capacity retention of the CoAl-MMO coated $LiMn_2O_4$ with cobalt loading of 2–4% after 50 cycles at 25 °C or 55 °C is higher than that of $Co_3O_4$ coated $LiMn_2O_4$. In addition, it was reported that $LiMn_2O_4$ coating with $Co_3O_4$ (a molar Mn/Co ratio is 10, so cobalt loading is 6.5 wt.% based on $LiMn_2O_4$ according to calculation) prepared by using methanol as solvent could significantly improve the electrochemical stability at elevated temperature [13]. However, there are few reports that $LiMn_2O_4$ coating with $Al_2O_3$ could significantly enhance the elevated temperature electrochemical performance. This paper describes that the CoAl-MMO coated $LiMn_2O_4$ prepared by co-precipitation method by using water as solvent could improve the elevated temperature electrochemical performance of $LiMn_2O_4$, and the cobalt loading amount could decrease to 3 wt.% based on $LiMn_2O_4$. This could be contributed to synergistic effects between cobalt and aluminum oxide species.

## 4. Conclusion

We have successfully prepared CoAl-MMO coated spinel $LiMn_2O_4$ in order to improve the electrochemical cycling behavior of the spinel material at elevated temperature. The effects of varying the calcination temperature and the amount of the CoAl-MMO coating have been investigated. The CoAl-MMO (3 wt.% Co and 0.5 wt.% Al based on $LiMn_2O_4$) coated $LiMn_2O_4$ after heat-treatment at 400 °C shows the best cycling stability, with a specific discharge capacity of 100 mAh $g^{-1}$ and 92.2 mAh $g^{-1}$ after 50 cycles at 25 °C and 55 °C, respectively. Enhancement of the electrochemical properties can be attributed to the surface coating of CoAl-MMO, giving rise to blocking the direct contact between the spinel and electrolyte, which inhibits both decomposition of the electrolyte and dissolution of the spinel $LiMn_2O_4$ into the electrolyte. Coating the surface of $LiMn_2O_4$ with CoAl-MMO could be an effective way to improve its electrochemical performance at elevated temperatures in practical batteries.

## Acknowledgments

This work was supported by the National Natural Science Foundation of China, the Ministry of Science and Technology High Technology Development (863) Plan (Grant No. 2006AA03Z343), and the 111 Project (Grant No. B07004).

## References

[1] C.H. Shen, R.S. Liu, R. Gundakaram, J.M. Chen, S.M. Huang, J.S. Chen, C.M. Wang, J. Power Sources 102 (2001) 21–28.
[2] X. He, J. Li, Y. Cai, Y. Wang, J. Ying, C. Jiang, C. Wan, J. Power Sources 150 (2005) 216–222.
[3] Y.-K. Sun, K.-J. Hong, J. Prakash, K. Amine, Electrochem. Commun. 4 (2002) 344–348.
[4] S.-C. Park, Y.-S. Han, Y.-S. Kang, P.S. Lee, S. Ahn, H.-M. Lee, J.-Y. Lee, J. Electrochem. Soc. 148 (2001) A680–A686.
[5] D. Liu, X. Liu, Z. He, Mater. Chem. Phys. 105 (2007) 362–366.
[6] S.B. Park, S.M. Lee, H.C. Shin, W.I. Cho, H. Jang, J. Power Sources 166 (2007) 219–225.
[7] D. Liu, Z. He, X. Liu, Mater. Lett. 61 (2007) 4703–4706.
[8] H.-O. Ha, N.J. Yun, K. Kim, Electrochim. Acta 52 (2007) 3236–3241.
[9] T. Noguchi, I. Yamazaki, T. Numata, M. Shirakata, J. Power Sources 174 (2007) 359–365.
[10] H.-W. Chan, J.-G. Duh, S.-R. Sheen, S.-Y. Tsai, C.-R. Lee, Surf. Coat. Technol. 200 (2005) 1330–1334.
[11] H.-W. Chan, J.-G. Duh, H.-S. Sheu, J. Electrochem. Soc. 153 (2006) A1533–A1538.
[12] S.-W. Lee, K.-S. Kim, H.-S. Moon, H.-J. Kim, B.-W. Cho, W.-I. Cho, J.-B. Ju, J.-W. Park, J. Power Sources 126 (2004) 150–155.
[13] J. Cho, T.-J. Kim, Y.J. Kim, B. Park, Chem. Commun. (2001) 1074–1075.
[14] J. Tu, X.B. Zhao, G.S. Cao, D.G. Zhuang, T.J. Zhu, J.P. Tu, Electrochim. Acta 51 (2006) 6456–6462.
[15] J.-M. Han, S.-T. Myung, Y.-K. Sun, J. Electrochem. Soc. 153 (2006) A1290–A1295.
[16] D.G. Evans, X. Duan, Chem. Commun. (2006) 485–496.
[17] X. Duan, D.G. Evans, Struct. Bond. 119 (2006) 1–87.
[18] S. Komaba, K. Oikawa, S.-T. Myung, N. Kumagai, T. Kamiyama, Solid State Ionics 149 (2002) 47–52.
[19] D. Song, H. Ikuta, T. Uchida, M. Wakihara, Solid State Ionics 117 (1999) 151–156.
[20] R.S. Liu, C.H. Shen, Solid State Ionics 157 (2003) 95–100.
[21] T. Yi, X. Hu, K. Gao, J. Power Sources 162 (2006) 636–643.
[22] Y. Xia, H. Takeshige, H. Noguchi, M. Yoshio, J. Power Sources 56 (1995) 61–67.
[23] J.T. Son, H.G. Kim, Y.J. Park, Electrochim. Acta 50 (2004) 453–459.
[24] Y. Wang, W. Yang, S. Zhang, D.G. Evans, X. Duan, J. Electrochem. Soc. 152 (2005) A2130–A2137.
[25] K. Amine, J. Liu, S. Kang, I. Belharouak, Y. Hyung, D. Vissers, G. Henriksen, J. Power Sources 129 (2004) 14–19.
[26] B. Deng, H. Nakamura, M. Yoshio, J. Power Sources 180 (2008) 864–868.
[27] Y. Xia, T. Sakai, T. Fujieda, X.Q. Yang, X. Sun, Z.F. Ma, J. McBreen, M. Yoshio, J. Electrochem. Soc. 148 (2001) A723–A729.
[28] B. Deng, H. Nakamura, M. Yoshio, Chem. Lett. 32 (2003) 942–943.